High Voltage Electron Microscopy

Proceedings of the Third International Conference

edited by

P. R. SWANN

Department of Metallurgy and Materials Science, Imperial College, London

C. J. HUMPHREYS and M. J. GORINGE

Department of Metallurgy and Science of Materials, Oxford

1974

Academic Press: London and New York

A Subsidiary of Harcourt Brace Jovanovich, Publishers

THE CRITICAL VOLTAGE EFFECT AND ITS APPLICATIONS

by L. E. Thomas, C. G. Shirley, J. S. Lally, and R. M. Fisher

1. Introduction

One of the unexpected many-beam diffraction phenomena discovered in the HVEM (Nagata and Fukuhara 1967; Uyeda 1968), the critical voltage effect allows considerable refinement of atom form factors (Watanabe *et al.* 1968) and Debye temperatures (Lally *et al.* 1972) appropriate to electron diffraction, the determination of long-range order, microsegregation, and local atomic displacements in alloys (Lally *et al.* 1972), and, probably, further applications in non-metallic crystals. The information thus provided is unique, moreover, in being related to the microscopic volume sampled by an electron probe 1 μm or less in diameter. This paper summarizes recent developments in critical voltage methods and applications and includes useful compilations of V_C values and refined scattering data for a large number of frequently studied elements. Instead of using a single V_C value to find the atom form factor $f(s)$, $s = \sin\theta/\lambda$, appropriate to one scattering angle, as previously, the use of two V_C values allows f to be redetermined over the entire range of scattering angles corresponding to low-index Bragg reflections. These new scattering data, along with a theoretical analysis of electron scattering from disordered alloys provide the basis for extracting information about atomic binding and short-range order (SRO) from V_C measurements.

For present purposes a critical voltage is defined as an electron accelerating voltage where two of the Bloch waves associated with the row of reflections mg (integer m) from one set of crystal planes become degenerate due to many-beam interactions. Several such effects, each marking the onset of either three-, four- or five-beam systematic interactions, have been found, and each is associated with several characteristic changes in diffraction behaviour which may be observed on any electron diffraction pattern or image that reveals the variation in diffracted intensity with crystal orientation (Thomas 1972). Fig. 1(a) illustrates via Kikuchi (K) patterns the two most prominent indicators of the familiar 'second-order' critical voltage effect associated with waves 2 and 3 (labelled in order of increasing wavevector): the vanishing of the second-order K-lines and the asymmetry reversal of the 000 K-line. Corresponding effects, related to the K-pattern behaviour by reciprocity (Thomas 1972) appear on bend contour images and convergent beam patterns. The third-order critical voltage effect shown in Fig. 1(b) is limited to systematic diffraction cases where the structure factors F_{mg} are mixed in character, such as 111 diffraction from diamond cubic crystals and 100 diffraction from hcp crystals. Similarly, critical-voltage effects involving the disappearance of fourth-order reflections are exhibited by ordered crystals when both superlattice and fundamental reflections are excited. Such higher-order effects are not found for

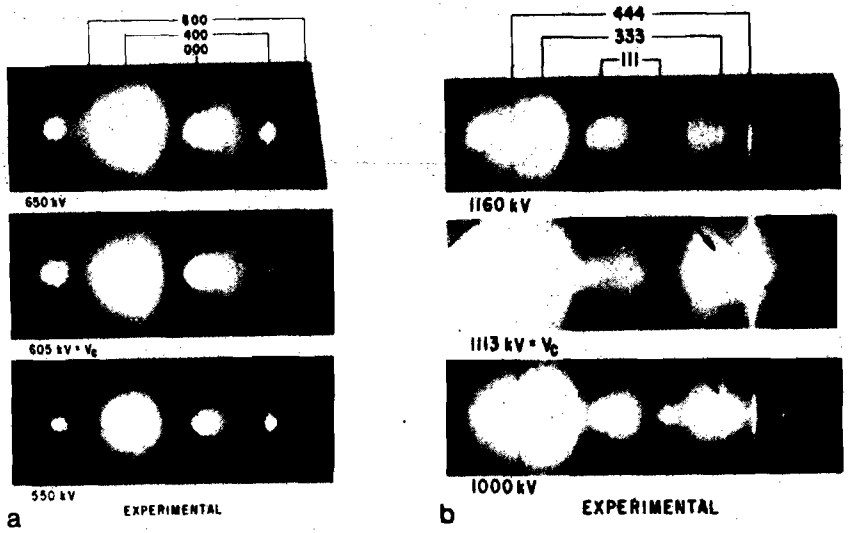

Fig. 1. Kikuchi patterns showing the (a) second-order and (b) third-order critical voltage effect.

simple fcc or bcc metals. Orientation-dependent Bloch wave degeneracies may also occur due to 'accidental' interaction of non-systematic reflections and, as shown by Gjønnes and Høier (1972), these can be also used to refine scattering factors. However, non-systematic effects are excluded here except as a perturbation of the systematic case.

2. Methods

Although critical voltages are found usually by observing the disappearance voltage for second-order K-lines or second-order Bragg maxima on bend-contour images, the abrupt asymmetry reversal of the 000 K-line at V_C (Fig. 1(a)) is a superior indicator which allows V_C to be bracketed rapidly and which avoids the uncertainty inherent in determining a shallow intensity minimum. With suitably thick and perfect crystals, the asymmetry reversal method can locate V_C reproducibly with ± 0.5 per cent compared with ± 1 per cent for disappearance methods. Compared with bend-contour and convergent-beam images, K-patterns also offer the advantage of suppressing thickness oscillations of diffracted intensity and of ensuring the use of relatively perfect crystal regions. Third- and fourth-order critical voltages can be determined similarly from the sense of asymmetry of the respective first- and second-order K-lines.

3. Theory

Critical voltages can also be determined exactly from theory simply by examining the relevant Bloch wave excitation coefficients $C_0^{(j)}$ obtained from the usual matrix formulation. For the second-order effect

$$V < V_c \text{ if } |C_0^{(2)}| > |C_0^{(3)}|$$

and

$$V > V_c \text{ if } |C_0^{(3)}| > |C_0^{(2)}|$$

for a crystal setting of $k_g = 0$ (the symmetry position).
Similarly, for third-order critical voltages the criterion is

$$V > V_c \text{ if } |C_0^{(3)}| < |C_0^{(4)}|$$

and

$$V < V_c \text{ if } |C_0^{(3)}| > |C_0^{(4)}|$$

at $k_g = 0.5$ (first-order Bragg position).

Thus V_c can be calculated rapidly by iteration, using the immediate result of a single matrix diagonalization at each step. For more complex diffraction cases it is necessary to examine the Bloch wave behaviour for each situation in order to choose the appropriate $|C_0^{(j)}|$ values. These criteria were established by examining the general Bloch wave behaviour which coincides with the systematic degeneracy of waves 2 and 3 and 4 at all even- or all odd-order Bragg positions respectively. Our many-beam calculations also have shown that the applicability of these rules is the same whether or not absorption is included explicitly, and also that the 000 K-line asymmetry reversal and the other observable indicators of critical voltages coincide exactly with the Bloch wave degeneracies so long as thickness oscillations of diffracted intensity are suppressed.

Since the effect of non-systematic reflections is usually not considered in critical voltage calculations, it is important in practice to choose systematic crystal orientations where non-systematic interactions are negligible. Such orientations, lying midway between medium-low index crystal directions, are easily recognized from K-patterns, as in Fig. 2. To illustrate the effect of non-systematics, V_c has been calculated for this 200 systematic case as a function of angular deviation from the [012] orientation, taking into account up to 30 Bragg reflections from this zone axis for each orientation investigated. The results, also given in Fig. 2, indicate the importance of avoiding exact zone-axis orientations as well as locations where important non-systematic K-lines intersect the systematic K-lines of interest.

A great advantage of critical voltage methods lies in the fact that V_c can be calculated exactly from many-beam dynamical theory using only the relevant set of temperature-corrected structure factors F_{mg} and the spacing of the diffracting planes $\left|\frac{1}{g}\right|$. It is common in electron diffraction to express the structure factors in

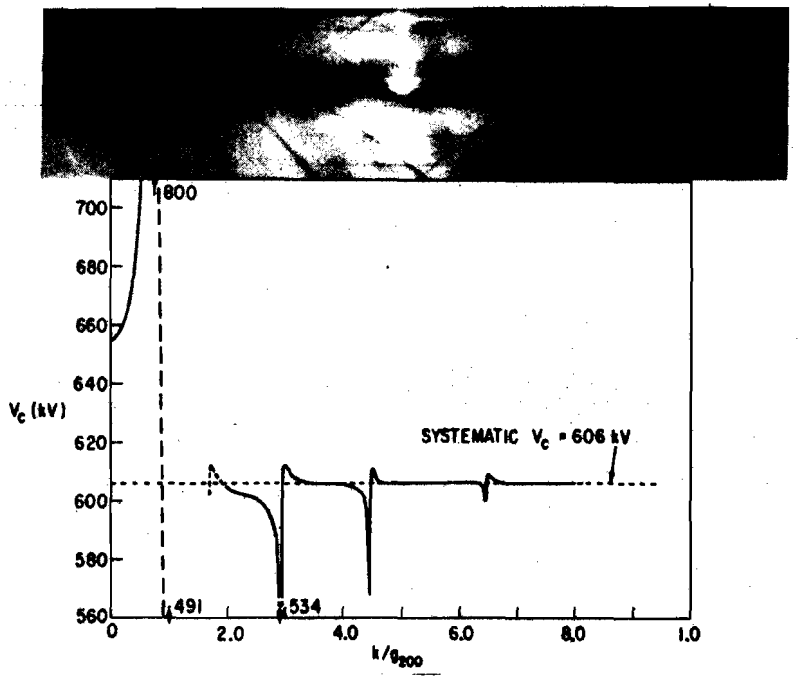

Fig. 2. Orientation-dependence of V_C near [012] in copper.

terms of 'two-beam extinction distances'

$$\xi_g = \pi\Omega_c/\lambda F_g = \pi\Omega/\lambda \sum_{\text{unit cell}} f_j \exp(2\pi i\, g \cdot r_j) \quad , \qquad (1)$$

where Ω_c is the unit cell volume and λ is the relativistic electron wavelength. The atom form factors in this expression are usually obtained from one of the various theoretical tabulations for free atoms at rest, and require temperature correction

$$f(s)_{\text{thermal}} = f_0 \exp(-Bs^2) \quad , \qquad (2)$$

where the temperature factor B is related to the mean squared atomic displacements $\langle u^2 \rangle$ and the Debye temperatures θ_D as

$$B = \frac{8\pi^2}{3}\langle u^2 \rangle = \frac{11492\phi(\theta/T)}{\mu\theta_D^2} + \frac{2873}{\mu\theta_D} \quad , \qquad (3)$$

and where μ is the atomic weight and ϕ is the Debye function.

4. Measurements of atom form factors

Previous critical-voltage calculations of atom form factors f have used a single V_C value to adjust $f(g)$, accepting as accurate $f(mg)$, $m \geqslant 2$, given by one of the various theoretical free-atom models. To improve the method, we measured V_C for at least two systematic cases for each metal and used these to adjust the entire f versus $\sin\theta/\lambda$ curve at low angles rather than just one point. Since many metals yielded only one room temperature V_C value within our range of 20-1150 kV, a heating stage was sometimes used to lower V_C. These determinations gave θ_D as a by-product. Fig. 3 outlines the main steps of the computer programme used to refine f values.

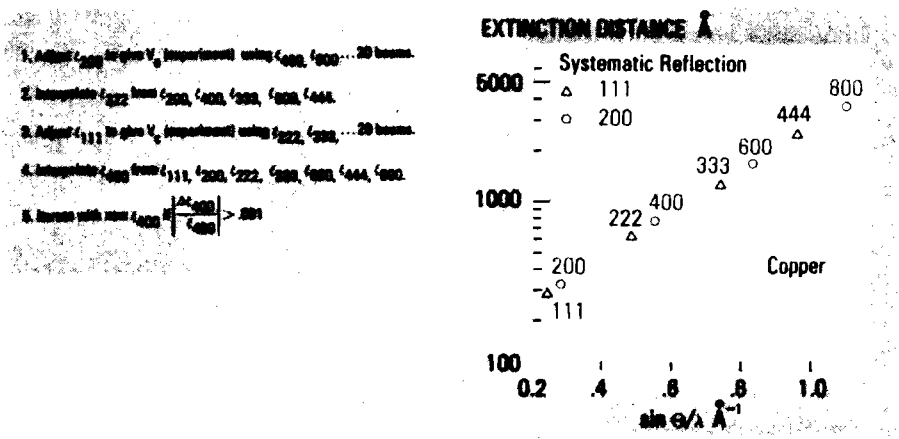

Fig. 3. Scheme for refining low-index extinction distances from V_C values.

Before applying these correction procedures, however, measured critical voltages were compared with V_C values predicted using various theoretical atom form-factor tabulations. As indicated by the results for fcc metals given in Fig. 4, the most sophisticated of the atomic models investigated, the relativistic Hartree-Fock model tabulated by Doyle and Turner gave the best predictions. RHF atom form factors were therefore used as the basis for further corrections. Fig. 5 contrasts the corrected scattering data for fcc metals (given for convenience here as temperature-corrected two-beam extinction distances) with Smith-Burge extinction distances from Hirsch *et al.* (1965). It should be pointed out that differences arising from the scattering models used are much greater than the corrections introduced. Figs. 6 to 9 list critical voltages determined for bcc, hcp, and diamond cubic crystals, as well as some of the refined extinction distances.

Figs. 4-9. Experimental critical voltages and refined extinction distances. Note: V_c values in ( ) are predicted from refined scattering data.

Critical Voltages For FCC Metals

Element	θ_D	Reflection	Thomas-Fermi-Dirac	Self-Consistent Field	Relativistic Hartree-Fock	Expt. @22°C
13 Al	395 °K	111	-	471 KV	472 KV	425[2], 430[3] KV
		200	-	993	987	918±5, 895[1]± 15
27 Co	380	111	144	296	280	276±2
		200	-	-	547	555±3
		220	-	-	1758	(1745)
		311	-	-	2683	(2686)
28 Ni	390	111	122	325	305	295[3], 298±2
		200	398	599	602	588±3, 587[1]±20
		220	1647	1808	1808	(1794)
		311	2815	2680	2732	(2730)
29 Cu	320	111	106	420	400	310[2], 325[1], 310±3
		200	352	629	674	600[2], 605±3
		220	1473	2012	1788	(1750) 1750[6]±50
		311	2437	2276	2600	(2587) 2700[6]±75
47 Ag	220	111	<0	23	71	55[4]
		200	178	175	238	225[2]
		220	997	844	936	919±5
		311	1650	1411	1510	(1498)
79 Au	185	111	<0	-	<0	-
		200	22	-	113	108±2
		220	639	-	734	726±5
		311	1149	-	1275	(1286)
		331	2387	-	2817	-

Fig. 4.

TWO BEAM EXTINCTION DISTANCES $\xi_g = \pi \Omega_{cell} \cos \theta_B / \lambda F_g$ from Hirsch et al AND FROM RHF VALUES AFTER CORRECTION FOR TEMPERATURE AND V_c EFFECT

Reflection	Al		Ni		Cu		Ag		Au	
	Hirsch et al	this work								
111	(556)Å	563.2	(236)	267.8	(242)	285.6	(224)	241.6	(159)	182.5
200	(673)	684.9	(275)	308.7	(281)	326.3	(256)	271.5	(179)	202.4
220	(1057)	1143.9	(409)	445.7	(416)	472.5	(363)	385.8	(248)	278.1
311	(1300)	1476.3	(499)	547.1	(508)	579.0	(433)	473.8	(292)	336.3
222	(1377)	1586.2	(529)	581.1	(535)	615.0	(466)	504.0	(307)	358.9
400	(1672)	2024.0	(652)	720.0	(654)	763.7	(544)	630.1	(363)	435.0
331	(1877)	2356.9	(745)	829.2	(745)	881.4	(611)	729.7	(406)	494.6

Fig. 5.

[1] Arii, T. and Uyeda, R. (1969). *Japan. J. appl. Phys.*, 8, 621; also, Arii, T., Uyeda, R., Terasaki, O., and Watanabe, D. (1973). *Acta Crystallogr.* A29, 295.
[2] Lally *et al.* (Ref. 4 this paper).
[3] Watanabe, D., Uyeda, R., and Fukuhara, A. (1969). *Acta Crystallogr.* A25, 138.
[4] Fukuhara, A. and Yanagisawa, A. (1969). *Japan. J. appl. Phys.*, 8, 1166.
[5] Fujimoto, M., Terasaki, O., and Watanabe, D. (1972). *Phys. Lett.*, 41A, 159.
[6] Rocher, A. and Jouffrey, B. (1972). *C.r. hebd. Séanc. Acad. Sci., Paris* 275, 133.

CRITICAL VOLTAGES FOR BCC METALS

Element	θ_D	Reflection	Relativistic Hartree-Fock	Expt. ● 22°C	High Temperature Measurements
23 V	°K 390	110 200 211	277 1240 2260	238[5], 230 ± 2.5 kv - -	
24 Cr	495 (Exp)	110 200 211	336 1266 2297	259[5], 265 ± 1.5 (1238) predicted -	215 ± 1.5 ● 385°C 1088 ± 5 ● 385°C
26 Fe	425 (Exp)	110 200 211	331 1299 2319	305[3,2] (1249) -	254 ± 3 ● 295°C 1099 ± 5 ● 295°C
41 Nb	265	110 200 211	68 747 1550	35 ± 3 749 ± 3 (1595)	
42 Mo	380	110 200 211	74 790 1682	35 ± 3 789 ± 2 (1729)	752 ± 2 ● 268°C
73 Ta	230	110 200 211 310	29 650 1316 2757	- 651 ± 2 (1316) -	
74 W	315	110 200 211	22 662 1365	660 ± 3 >1100 (1365)	

Fig. 6.

CRITICAL VOLTAGES FOR hcp METALS

Element	θ_D	Reflection	Relativistic Hartree-Fock	Expt. ● 22°C
4 Be	°K 1000	00.2 $\bar{1}$1.1 $\bar{1}$1.0, $\bar{1}$12	1256 KV 709 < 0	- 718 ± 10 KV -
12 Mg	330	00.2 $\bar{1}$1.1 $\bar{1}$1.0	733 348 < 0	678 ± 6 310 ± 5 ≪ 100
22 Ti	355	00.2	277	236[1]
27 Co	380	00.2 $\bar{1}$1.1 11.0 $\bar{1}$1.0	286 2 1746 < 0	280[2], 278 ± 2 ≪ 100 - ≪ 100

Fig. 7.

CRITICAL VOLTAGES FOR hcp METALS

Element	θ_D	Reflection	Relativistic Hartree-Fock	Expt. @ 22°C
4 Be	$\frac{\theta_X}{1000}$	00.2	1256 kV	-
		11.1	709	718 ± 10 kV
		11.0, 12	< 0	-
12 Mg	330	00.2	733	678 ± 6
		11.1	348	310 ± 5
		11.0	< 0	<< 100
22 Ti	386	00.2	277	235[1]
27 Co	380	00.2	286	280[2], 278 ± 2
		11.1	2	<< 100
		11.0	1746	-
		11.0	< 0	<< 100

Fig. 8.

DIAMOND CUBIC CRYSTALS

Element	Refl.	Experimental Critical Voltages	
14 Si	111	V_c(3) 1113 ± 6 kv	V_c(3) 991 ± 9 @ 815°C
	220	> 1130	1101 ± 6 @ 815°C
32 Ge	111	926 ± 6 V_c(3)	
	220	1028 ± 9	
	400	> 1100	
Ga P	111	V_c(3) 1026 ± 5	
	220	1098 ± 5	
	400	> 1100	

Fig. 9.

5. Critical-voltage applications in alloys

The critical voltage of alloys is affected by physical parameters that do not pertain to pure metals. Long-range order, for example, can increase the critical voltage over the disordered state (see Fig. 10), although the effect is smaller than

Cu_3Au (24.4 at. % Au)

Reflection	Temp. (°C)	V_c (s = 1)	V_c (s = 0)	B(s = 1)	B(s = 0)
(111)	25	175½3(188)	166±2(188)	.62	.60
(200)	25	425±3(468)	381±3(420)	.89	.63
(200)	188	364±2 -	- -	.55	-

Critical voltages in kv; values in ( ) predicted theoretically using RHF atom form factors.

Fig. 10. Long-range order on V_C in Cu_3Au. Note revised values (Lally *et al.* 1972).

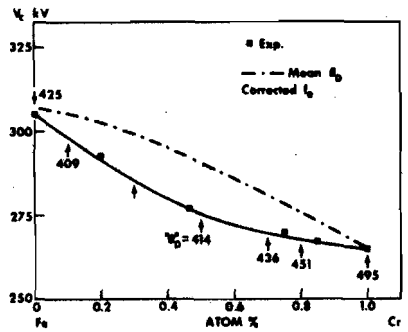

Fig. 11. Predicted and measured V_C values for Fe-Cr, showing calculated alloy Debye temperatures.

was previously believed (Lally *et al.* 1972). As shown in Figs. 11 and 12, however, measured critical voltages for disordered alloys are often considerably less than would be expected if the electron scattering behaviour of the alloy is a simple mean of scattering factors for the pure elements. Since alloying apparently has little effect on the atom form factors themselves, the differences between theory and experiment must arise from the effects of atomic force constant changes, lattice strains, and short-range order (SRO) on mean squared atomic displacements in the alloy; i.e. through effective temperature factors which can be calculated directly from f values for the end member atoms and V_C values for the alloys. The following summarizes a theoretical analysis of such pseudo-temperature effects (Shirley 1973) for the Fe-Cr system, which is believed to represent a strain-free, random alloy at all compositions, and the Au-Ni system, which includes strain effects and, at certain

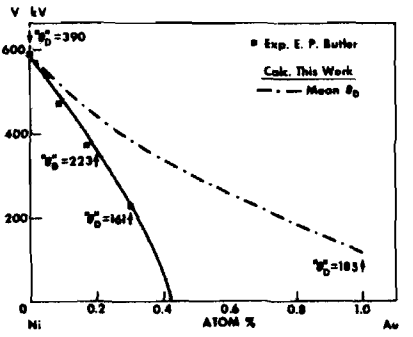

Fig. 12. V_C for Ni-Au, experimental data from Butler (1972).

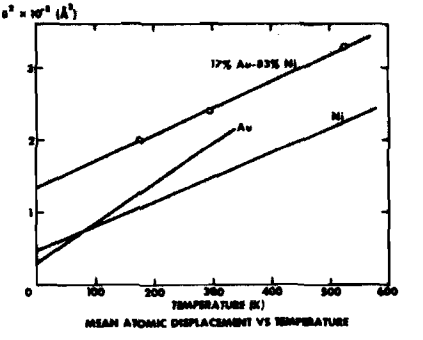

Fig. 13.

compositions, has a tendency to segregate.

The analysis assumes that the mean squared atomic displacements in alloys can be separated into a time-dependent (or thermal) part and a static (or strain) part as

$$\langle \omega^2 \rangle = \langle \omega_t^2 \rangle + \langle \omega_s^2 \rangle \quad , \tag{4}$$

where $\langle \omega_t^2 \rangle$ is given by eqn (3), with

$$\mu\theta^2 = m_A\mu_A\theta_A^2 + m_B\mu_B\theta_B^2 + (1-\tau)(1-\alpha_1)\, m_A m_B\, (\mu_A\theta_A^2 + \mu_B\theta_B^2) \quad , \tag{5}$$

for an alloy of A and B atoms, where now in eqns (5) and (3), $\mu = m_A\mu_A + m_B\mu_B$. The quantities m_A and m_B are the mole fractions of A atoms and B atoms, and θ_A and θ_B are the pure-metal Debye temperatures. Here α_1 is the nearest-neighbour Cowley-Warren SRO parameter and

$$\tau = \frac{2q^{AB}}{q^{AA} + q^{BB}} \quad , \tag{6}$$

where q is an effective interatomic force constant. Thus for Fe-Cr, if we assume $\alpha_1 = 0$ and no strain effects appear, the theory reduces to one parameter τ, which yields an average value of 0.58 consistent with the pseudo-Debye temperatures found at each composition. Taken at face value this indicates that the Fe-Cr bond is about 0.6 times less stiff than the Fe-Fe and the Cr-Cr bonds.

The effect of the strain arising from differences in atomic radii is to introduce a static displacement

$$\langle \omega_s^2 \rangle = \frac{1}{4}\, m_B m_A \gamma^2 \left| \frac{da}{dm_A} \right|^2 \quad (0.5 + 2.6\,\alpha_1 + \text{other SRO terms}),$$

where a is the lattice parameter and γ is an empirically determined, composition-

independent constant. For Ni-17% Au, the effects of thermal vibration and static strains can be separated by measuring critical voltages at different temperatures as well as different compositions, since the strain effects are effectively independent of temperature, as shown in Fig. 13. Analysis of $\langle u^2 \rangle$ obtained for this alloy at several temperatures yields average values of $\tau = 2.4$ and $\gamma = 1.52$, assuming $\alpha_1 = 0$. These values for τ and γ, however, predict $\langle u^2 \rangle$ for a Ni-30% Au alloy substantially smaller than that obtained from the corresponding critical-voltage measurement. The difference can be accounted for by assuming $\alpha_1 = 0.22$ in the Ni-30% Au alloy, which is consistent with its known behaviour as a segregating system. This work, although preliminary, indicates that the critical-voltage technique, with its practical convenience, sensitivity, and microscopic applicability may also be useful for studying SRO kinetics.

It seems clear at this point that additional critical-voltage effects, corresponding to different Bloch wave degeneracies, remain to be discovered and that further important applications will appear for complex crystals. The methods and results described here should be useful for exploring such effects.

6. References

Butler, E. P. (1972). *Phil. Mag.* **26**, 33.

Gjønnes, J. and Høier, R. (1972). *Acta. Crystallogr.* A**27**, 313.

Hirsch, P. B., Howie, A., Nicholson, R. B., Pashley, D. W., and Whelan, M. J. (1965). *Electron Microscopy of Thin Crystals*, Butterworth, London.

Lally, J. S., Humphreys, C. J., Metherell, A. J. F., and Fisher, R. M. (1972). *Phil. Mag.* **25**, 321.

Nagata, F. and Fukuhara, A. (1967). *Japan. J. appl. Phys.* **6**, 1233.

Shirley, G. C. (1973). Ph.D. Thesis, Arizona State University.

Thomas, L. E. (1972). *Phil. Mag.* **26**, 1447.

Uyeda, R. (1968). *Acta. Crystallogr.* A**24**, 175.

Watanabe, D., Uyeda, R., and Kogiso, M. (1968). *Acta Crystallogr.* A**24**, 249.